REPORT DOCUMENTATION PAGE

Form Approved
OMB No. 0704-0188

1. AGENCY USE ONLY (Leave blank)	2. REPORT DATE	3. REPORT TYPE AND DATES COVERED
	July 18, 1996	Technical

4. TITLE AND SUBTITLE
Dispersion and dipolar orientational effects on the linear electro-absorption and electro-optic responses in a model guest/host nonlinear optical system

5. FUNDING NUMBERS
#313H030
Kenneth J. Wynne

6. AUTHOR(S)
T. Goodson III and C. H. Wang

7. PERFORMING ORGANIZATION NAME(S) AND ADDRESS(ES)
632 Hamilton Hall
Department of Chemistry
University of Nebraska-Lincoln
Lincoln, NE 68588-0304

8. PERFORMING ORGANIZATION REPORT NUMBER
7

9. SPONSORING / MONITORING AGENCY NAME(S) AND ADDRESS(ES)
Office of Naval Research
800 N. Quincy Street
Arlington, VA 22217-5000

10. SPONSORING/ MONITORING AGENCY REPORT NUMBER
Office of Naval Research

11. SUPPLEMENTARY NOTES
Journal of Applied Physics, submitted

12a. DISTRIBUTION/AVAILABILITY STATEMENT
Distribution Unlimited

12b. DISTRIBUTION CODE
Unlimited

13. ABSTRACT, *(Maximum 200 words)*

Linear electro-absorption (LEA) and linear electro-optic (LEO) measurements are demonstrated using a model guest/host system consisting of disperse red 1 (DR1) doped in poly(methyl)methacrylate (PMMA). The LEA response is measured over a wavelength range of 300-700 nm. Electro-optic measurements of the real and imaginary parts of the electric field induced Pockels coefficient are carried out at wavelengths near and far from the resonant absorption. A shift in the absorption maximum and change in the bandshape of the LEA spectrum are related to the linear Stark effect and dipolar orientation. Expressions for the real and imaginary parts of the Pockels coefficient derived from the two experiments are provided. Induced dipolar order as a result of the contact poling process is investigated by the LEA measurement. Information concerning the relaxation of the induced dipolar order, investigated by the LEA measurement, is compared to the relaxation results obtained by the second harmonic generation technique.

14. SUBJECT TERMS	15. NUMBER OF PAGES
	24
	16. PRICE CODE

17. SECURITY CLASSIFICATION OF REPORT	18. SECURITY CLASSIFICATION OF THIS PAGE	19. SECURITY CLASSIFICATION OF ABSTRACT	20. LIMITATION OF ABSTRACT
Unclassified	Unclassified	Unclassified	Unlimited

Dispersion and dipolar orientational effects on the linear electro-absorption and electro-optic responses in a model guest/host nonlinear optical system

T. Goodson III and C.H. Wang*
Department of Chemistry, University of Nebraska-Lincoln
Lincoln, NE 68588-0304

* Author to whom all correspondence should be sent.

Abstract

Linear electro-absorption (LEA) and linear electro-optic (LEO) measurements are demonstrated using a model guest/host system consisting of disperse red 1 (DR1) doped in poly(methyl)methacrylate (PMMA). The LEA response is measured over a wavelength range of 300-700 nm. Electro-optic measurements of the real and imaginary parts of the electric field induced Pockels coefficient are carried out at wavelengths near and far from the resonant absorption. A shift in the absorption maximum and change in the bandshape of the LEA spectrum are related to the linear Stark effect and dipolar orientation. Expressions for the real and imaginary parts of the Pockels coefficient derived from the two experiments are provided. Induced dipolar order as a result of the contact poling process is investigated by the LEA measurement. Information concerning the relaxation of the induced dipolar order, investigated by the LEA measurement, is compared to the relaxation results obtained by using the second harmonic generation technique.

Introduction

Nonlinear optical (NLO) and linear electro-optical (EO) materials have attracted great interest due to the possibility of their use in opto-electronic applications.[1-5] Originally inorganic crystals such as $LiNbO_3$ and KH_2PO_4 had been used as nonlinear optical materials. The need for more versatile and thermally stable materials gave rise to the use of organic polymeric systems. Extensive experimental and theoretical studies were performed in order to characterize the NLO properties of organic polymeric materials.[6-10] Primarily, these investigations were concerned with the magnitude and the temporal stability of the second order susceptibility, $\chi^{(2)}$, measured by the second harmonic generation technique.[11-13]

In the case of amorphous polymeric materials, no significant second order effect could be achieved without considering the electric field poling process. Poling the organic polymeric material can be accomplished by raising the temperature of the polymeric system above its glass transition temperature, T_g, while simultaneously applying a large static electric field. After an equilibrium is obtained, the temperature is lowered below T_g, and the field is turned off. Unfortunately, after the removal of the electric field the induced orientational order tends to decay over time and the second order effect gradually reduces to zero. To overcome this problem certain functionalized systems[14-15] and guest/host systems with high T_g host polymers[16,17] have been used; however the problem of increasing the NLO activity and enhancing temporal stability has not been solved. There is a need to investigate the dynamics of the poling process and the effect of the poling field on SHG relaxation for various polymer systems before the development of a useful NLO polymeric material with

large and stable optical nonlinearities is accomplished.

Another quantity that characterizes the second order susceptibility of NLO polymeric materials is the linear electro-optic coefficient r (also known as the Pockels coefficient).[18] In the linear electro-optic effect a modulated (AC) electric field is applied to the polymer film causing a change in the index of refraction, proportional to the electric field. In general, the electro-optic coefficient is a third rank tensor, which is related to the second order susceptibility by[19]

$$r_{ijk} = \frac{-4}{n_j^2 n_k^2} \chi^{(2)}_{ijk}(-\omega ; \omega , 0) \qquad (1)$$

where r_{ijk} is the ijk'th component of the linear electro-optic tensor and $\chi^{(2)}_{ijk}$ is the corresponding component of the second order susceptibility tensor. The characterization of the real part of the linear electro-optic effect is normally performed by using a Mach-Zehnder interferometer. Unfortunately, this technique gives only single values of the real part of the Pockels coefficient at a fixed wavelength. This limitation excludes considerations of the important resonant contributions experienced when measurements are taken close to the maximum of the charge transfer absorption band. Consequently, many reports in the literature have excluded the resonant contribution and the imaginary part of the Pockels coefficient altogether.

Due to the dominance of the charge transfer state a relationship using a two level model that equates the electro-optic coefficient to the second order susceptibility at a different optical frequency has obtained some success. This relationship is given as,[20]

$$\left|\frac{r_{13}}{d_{13}}\right| = \frac{4}{n^4(\omega)} \times \frac{f^{\omega} f^{\omega} f^{0}}{f^{2\omega'} f^{\omega'} f^{\omega'}} \times \frac{(3\omega_0^2 - \omega^2)\ (\omega_0^2 - \omega'^2)\ (\omega_0^2 - 4\omega'^2)}{3\omega_0^2\ (\omega_0^2 - \omega^2)^2} \qquad (2)$$

where ω' is the frequency of the fundamental used in measuring d_{13} (which is simply $\chi^{(2)}/2$) and ω is the frequency that the electro-optic coefficient is evaluated. f^{ω} is the Lorentz local field factor at frequency ω given by $(n_{\omega}^2+2)/3$. f° is the local field factor at zero frequency, and in terms of Onsager's theory it is given by $\epsilon(n^2+2)/(n^2+2\epsilon)$. Here ϵ is the DC dielectric constant. This simplified two level description assumes both r_{ijk} and $\chi^{(2)}_{ijk}$ are both totally real. This is, in general, not true when measurements are made near the resonant absorption. To completely characterize the second order NLO properties of the organic material one must also consider the contribution from the imaginary part of both r_{ijk} and $\chi^{(2)}_{ijk}$. Thus, a more versatile and accessible technique is needed to yield the complete characterization of the second order susceptibility of polymeric materials involving charge transfer chromophores.

In this manuscript we develop a technique using the linear electro-absorption and electro-optic effects to characterize both the real and imaginary parts of the electro-optic coefficient and also examine the effect of the dispersion. We use a model guest/host system consisting of Disperse Red 1 (DR1) doped in amorphous poly(methyl)methacrylate (PMMA) to illustrate the technique. The linear electro-absorption response is measured over a wavelength range of 300-700 nm. The real part of the electro-optic coefficient is measured

at wavelengths near and far from the resonant absorption. Expressions for the real and imaginary parts of the linear electro-optic coefficient obtained by the experimental method are provided. Orientational order is induced in the guest/host system by a contact electrode poling technique. The decay of the induced dipolar order is investigated by the LEA measurement and the result is compared to the relaxation behavior as probed with the electric field induced second harmonic generation technique. We show that the LEA measurement can be used as a versatile tool in characterizing the second order nonlinear optical properties of organic polymeric materials near resonance.

Experimental

Appropriate amounts of the chromophore, Disperse Red 1 (DR1) (Aldrich 34,420-6) whose chemical structure is shown in Fig.1 and poly(methyl)methacrylate (PMMA) were dissolved in chloroform forming a 2.5 wt% solution. The solution was filtered to remove undissolved particulates. The amount of chloroform in solution was adjusted by evaporation to give a desired viscosity suitable for spin coating. Films were prepared by spin coating the polymer solution on soda lime glass slides, which were precoated with 300 Å SiO_2 and 250 Å ITO (indium tin oxide) films. The film/ITO sample assembly was placed in a vacuum oven first at 40 °C for over 24 hours and then baked at a temperature slightly above the glass transition. After certifying the chromophore concentration, one film/ITO slide was then placed on top of another to form a sandwich assembly. The assembly is then placed in a oven with the temperature set above the T_g of the polymer film to facilitate the fusion of two polymer films.

The refractive index and the thickness of the sample were determined by a prism coupler (Metricon) modified for a multiple wavelength operation. The prism coupler is operated in accordance with the optical waveguide principle where the polymer film serves as the propagation layer in the slab waveguide configuration.[21] Linear absorption (LA) and linear electro-absorption (LEA) measurements were performed with an apparatus constructed in our laboratory and is shown in Fig. 2. It includes the use of a 150 W xenon arc lamp, a monochromator, a stepper motor, a set of focusing lenses, polarizers, a chopper, and a set of Si diode detectors. The intensity of the transmitted light was detected by a photo-diode which was read by a lock-in amplifier. Another lock-in amplifier was also used to detect a part of the incident intensity used as a reference. The lock-in amplifiers, stepper motor, chopper, and monochromator were interfaced to and controlled by a PC. A modulated electric field was applied to the polymer film assembly by the use of a voltage amplifier. The modulated frequency of the applied field was 2 kHz for the LEA measurements reported here .

The absorption spectrum of a 2.5 wt % DR1/PMMA obtained by scanning the monochromator over a range of 300-700nm is shown in Fig.3. The scanning rate was 0.5 nm/sec. The maximum is found at 495 nm. Calculation of the molar extinction coefficient from the absorption maximum at the resonant frequency gives a value of 1.7×10^5 (L/cm*mol). Because the imaginary part of the refractive index corresponds to the absorption spectrum, wavelengths in the range of 480-530 nm were used in most the LEA measurements.

To detect the LEA signal, we used a two beam apparatus as shown in Fig.2. We

simultaneously measured the voltage signal from the application of the applied electric field to the sample at the modulated frequency and also the chopped transmitted light intensity using two lock-in amplifiers. Such measurements were initially carried out to verify the linear dependence of the LEA signal with the magnitude of the applied field, and to eliminate artifacts. The LEA response was measured by scanning over wavelengths close to and far from the absorption maximum.

The LEO measurements were performed by a procedure similar to that previously reported by Goodson and Wang.[22] A Mach Zehnder interferometer was used to measure the phase difference of optical responses between two arms, where a relative phase modulation resulted in an intensity modulation. The result is used to determine the real part of the Pockels coefficient.

The second harmonic generation (SHG) experimental setup is shown in Fig. 4. A Nd:YAG laser, $\lambda = 1.06\ \mu m$, Q-switched (5-8 ns pulse width, at 10 Hz, 300 mJ per pulse) was used to measure the second order nonlinear susceptibility of the electric field poled NLO polymer film, which was mounted on a goniometer stage. The fundamental wave was blocked by a short-pass filter. The second harmonic signal, obtained in transmission, was selected. It was detected by a photomultiplier tube, and finally averaged by a boxcar integrator (Princeton Applied Research model 165). Triggering and data acquisition was controlled by an optical (photo-diode) trigger. The boxcar output and optical triggering device were interfaced to a PC.

Results and Discussion

A. The linear electro-absorption experiment

In the linear electro-absorption (LEA) experiment we are interested in the change in the imaginary part of the refractive index as a function of the applied field. This is expressed as

$$n_I = n_{0I} + \frac{(n_0^3 r)_I E}{2} \qquad (3)$$

where E is the strength of the external electric field; subscript I indicates the imaginary part; $(n)_I$ is the imaginary part of the refractive index, n_o is the refractive index with no applied field, r_I is the imaginary part of the optical Pockels coefficient tensor which is related to the second order susceptibility in accordance with Eq. (1). For brevity, subscripts of r indicating a specific tensor component are omitted in Eq. (3) and in subsequent equations. The variation of $(n_o^3 r)_I$ with optical wavelength is known as the linear electro-absorption spectrum (LEA).

As light propagates through an absorbing medium, it is attenuated. The transmitted light intensity as detected by using the experimental setup given in Fig.2 is,

$$I = (t_1 t_2)^2 E_o^2 \exp\left[\frac{-4\pi n_I l}{\lambda}\right] \qquad (4)$$

Here, t_1 and t_2 refer to the transmission coefficients of the front and back substrates respectively. E_o is the amplitude of the optical field, λ is the wavelength of light, and l is the physical path length of the light in the medium. The optical path length is related to the sample thickness by Snell's law

$$l = \frac{d}{\cos\theta_{int}} = \frac{d}{(1-\frac{\sin^2\theta_{ext}}{n_R^2})^{\frac{1}{2}}} \qquad (5)$$

where d is the sample thickness, and n_R is the real part of refractive index, which in the linear electro-optic effect is related to the real part of the Pockels coefficient similar to Eq.3, except for taking the real part. θ_{int} and θ_{ext} refer to the internal and external refraction angles respectively. By the substitution of Eqs.3 and 5 into Eq.4 and expanding the expression to first order in E, one finds

$$I = I_0 \exp\frac{-2\pi d}{\lambda}\left[\frac{(n_0^3 r)_I E}{[1-(\sin^2\theta_{ext})/n_{0R}^2]^{1/2}} \cdot \right.$$

$$\left.\left[1-\frac{\sin^2\theta_{ext}/n_{0R}^2}{[1-\sin^2\theta_{ext}/n_{0R}^2]}\frac{n_{0I}(n_0^3 r)_R}{n_{0R}(n_0^3 r)_I}\right]\right] \qquad (6)$$

where n_{oI} and n_{oR} are the imaginary and real parts of the zero field refractive index in the

absence of the external electric field (E=0). Here, I_o is the light intensity measured by the detector with no applied field, and is given by,

$$I_0 = (t_1 t_2)^2 E_0^2 \exp\left[\frac{-4\pi n_{0I} d}{\lambda} / (1 - \sin^2\theta_{ext}/n_{0R}^2)^{1/2}\right] \quad (7)$$

One can easily detect I_o as a function of incident angle θ_{ext}. The result is stored in the computer data file. Using the measured values of n_{oI} (at 520 nm the imaginary part of the refractive index with no field applied is equal to 0.692) and incident intensity, one can fit the detected I_o as a function of angle to Eq. (7). The result is shown in Fig. 5. The fit was rather satisfactory. The result provides accurate values of the external angle θ_{ext} and d for subsequent studies. As to be seen below, the value of $(n_o^3 r)_R/n_{oR}$ at wavelengths within the absorption band is considerably smaller than $(n_o^3 r)_I/n_{oI}$. Thus, if the factor $(n_o^3 r)_R/n_{oR}$ is small compared with $(n_o^3 r)_I/n_{oI}$, and also if the incident angle θ_{ext} is such that $\sin\theta_{ext} < n_{oR}/2^{1/2}$ then the last term inside the square brackets on the right hand side of Eq. (6) can be neglected . As a result, equation (6) simplifies to

$$I = I_0 \exp\left[\frac{-2\pi d (n_0^3 r)_I E}{\lambda} (1 + \frac{1}{2}\sin^2\theta_{ext}/n_{0R}^2)\right] \quad (8)$$

For an AC modulating electric field with E given by $E = \mathscr{E}\cos(\Omega t)$, one obtains from Eq. (8) the intensity corresponding to the Fourier component at Ω due to the application of the AC

electric field on the NLO polymer film as

$$I^{\Omega} = I_0 \left[\frac{2\pi V_{rms}\sqrt{2}\,(n_0^3 r)_I}{\lambda} \left(1 + \frac{1}{2}\left(\sin^2\theta_{ext}/n_{0R}^2\right)\right)\right] \quad (9)$$

where V_{rms} ($=<E^2>^{1/2} = \mathcal{E}/2^{1/2}$) is the root mean square voltage applied to the sample.

Thus, at a given V_{rms}, by detecting I^{Ω} at frequency Ω using an lock-in amplifier as a function of the optical wavelength and also knowing n_{oR} and incident angle θ_{ext}, one can use Eq. (9) to obtain the quantity $(n_o^3 r)_I$. The LEA spectrum or $(n_o^3 r)_I$ as a function of wavelength over the region of 350 to 700 nm is shown in Fig.6.

Shown in Fig.7 is the dependence of the linear electro-absorption signal on the applied AC field for a 2.5 wt% DR1/PMMA film. Prior to this measurement, the polymer film was first poled using a contact electrode poling method. For contact poling, the sample was heated in an oven in the vicinity of T_g (at 80 °C) and allowed to equilibrate. A large static electric field (about 10^6V/cm) was applied across the film to orient the NLO chromophores dispersed in the polymer matrix. After poling the sample for a sufficiently long time, the sample temperature was slowly lowered while the static field was maintained. The static field was finally removed when the film temperature was at the room temperature. The LEA measurements were subsequently made with this poled film at room temperature.

Comparing Fig.6 with Fig.3 (the linear absorption spectrum), one sees that the two spectra are not identical. The maximum in the LA spectrum is found at 495 nm while that of the LEA spectrum is at 475 nm. The half height at half maximum of the LA spectra is

much wider than that of the LEA spectrum. The difference between the LEA and LA spectra is due to the linear Stark effect and dipolar orientation.

The linear Stark effect is purely of an electronic origin.[24,25] This effect can be seen as due to a perturbation in the non-degenerate energy levels of the dipolar dopant molecules caused by the application of the external electric field. The mixing of states and the perturbed change in the energy levels gives rise to a shift in absorption frequency which is proportional to the applied electric field. The dipolar orientation of the NLO chromophores also affects the LEA spectrum. As a matter of fact, in the absence of orientational order of the NLO chromophores, the LEA vanishes. Due to the fact that the LEA measurement is related to the second order effect, the orientation of the NLO dipoles plays a significant role on the magnitude and dispersion of the LEA response. The orientational order induced by the contact poling technique also affects the energy levels and density of states as a result of dipole-dipole interactions, ultimately causing a shift and spectral linewidth in the absorption spectrum.

B. Electro-optic response

We can obtain the linear electro-optic coefficient by separating the imaginary part of the refractive index from the real part with no applied field. The complex refractive index is given by,[27]

$$n_0 = n_{0R} + i n_{0I} \qquad (10)$$

where n_{0R} and n_{0I} refer to the real and imaginary parts respectively. The complex Pockels coefficient is given by,[27]

$$r = r_R + i r_I \tag{11}$$

where r_R and r_I refer to the real and imaginary parts, respectively. Substituting Eqs. (10) and (11) into the expression for $(n_o^3 r)$ and after separating out the real and imaginary components, we have found

$$(n_o^3 r)_R = Re\,[n_0^3 r] = r_R n_{0R}^3 - 3 r_R n_{0R} n_{oI}^2 - 3 r_I n_{0R}^2 n_{0I} + r_I n_{0I}^3 \tag{12}$$

$$(n_o^3 r)_I = Im\,[n_0^3 r] = r_I n_{0R}^3 + 3 r_R n_{0R}^2 n_{0I} - 3 r_I n_{0R} n_{0I}^2 - r_R n_{0I}^3 \tag{13}$$

which in a matrix form is given by,

$$\begin{vmatrix} (n_0^3 r)_R \\ (n_0^3 r)_I \end{vmatrix} = \begin{vmatrix} (n_{0R}^3 - 3 n_{0R} n_{0I}^2) & (n_{0I}^3 - 3 n_{0I} n_{0R}^2) \\ (3 n_{0R}^2 n_{0I} - n_{0I}^3) & (n_{0R}^3 - 3 n_{0I}^2 n_{0R}) \end{vmatrix} \begin{vmatrix} r_R \\ r_I \end{vmatrix} \tag{14}$$

The solution for the real and imaginary Pockels coefficient can be obtained by inverting the matrix:

$$\begin{vmatrix} r_R \\ r_I \end{vmatrix} = \frac{1}{[\,(n_{0R}^3 - 3n_{0R}n_{oI}^2)^2 + (n_{0I}^3 - 3n_{0I}n_{0R}^2)^2\,]} \begin{vmatrix} (n_{0R}^3 - 3n_{0R}n_{0I}^2) & (3n_{0I}n_{0R}^2 - n_{0I}^3) \\ (n_{0I}^3 - 3n_{0R}^2 n_{0I}) & (n_{0R}^3 - 3n_{0R}n_{0I}^2) \end{vmatrix} \begin{vmatrix} (n_0^3 r)_R \\ (n_0^3 r)_I \end{vmatrix} \quad (15)$$

or

$$r_I = \frac{(n_0^3 r)_I (n_{0R}^3 - 3n_{0R}n_{0I}^2) + (n_0^3 r)_R (n_{0I}^3 - 3n_{0R}^2 n_{0I})}{(n_{0R}^3 - 3n_{0R}n_{0I}^2)^2 + (n_{0I}^3 - 3n_{0I}n_{0R}^2)^2} \quad (16)$$

$$r_R = \frac{(n_0^3 r)_R (n_{0R}^3 - 3n_{0R}n_{oI}^2) - (n_0^3 r)_I (n_{0I}^3 - 3n_{0R}^2 n_{0I})}{(n_{0R}^3 - 3n_{0R}n_{0I}^2)^2 + (n_{0I}^3 - 3n_{0I}n_{0R}^2)^2} \quad (17)$$

Following Eqs. (16) and (17), one can calculate the real and imaginary parts of the Pockels coefficient from the imaginary and real parts of $(n_0^3 r)$ which can be obtained respectively from the LEA and the electro-optic experiments using a Mach-Zehnder interferometer.[22,29]

Despite the fact that we could obtain the values for the imaginary part of the electro-optic effect, $(n_0^3 r)_I$, over the entire wavelength range of 300-700 nm, due to the lack of a tunable laser source needed for our Mach-Zehnder interferometer, we could only measure $(n_o^3 r)_R$ for three particular laser wavelengths at 488, 514.5, and 632.8 nm. Thus values for r_I and r_R were only obtained for these three wavelengths. Table I summarizes the results of the

real part of the refractive index (zero field) (obtained from the Metricon apparatus), the imaginary part of the refractive index (zero field), the imaginary ($n_0^3 r$) values (obtained from linear electro-absorption measurements), and the real ($n_0^3 r$) values (obtained from the linear electro-optic Mach Zehnder measurements), along with the r_R and r_I calculated values using Eqs. 16 and 17. Also seen in Table I are the calculated ratios a defined as,

$$a = \frac{2 n_{0I} (n_o^3 r)_R}{n_{0R} (n_o^3 r)_I} \tag{18}$$

From consideration of this ratio the approximation introduced in Eq. 6 can be evaluated. At 632.8 nm, which is the wavelength far from the resonant absorption of the 2.5 wt% DR1/PMMA film the ratio is equal to 0.28, at 488 nm it is 0.215, while the ratio is 0.087 at 514.5 mm, a wavelength close to the maximum of the resonant absorption. Since we are concerned with the LEA response near the absorption maximum the approximation introduced in obtaining Eq. 6 is justified.

C. Relaxation of the Linear Electro-Absorption Intensity

As was mentioned above, the presence of dipolar order is a requirement for organic polymeric materials to exhibit second order NLO effects. The dipolar orientational order is induced by the poling process involving the use of a strong static electric field. However, the induced orientational order is relaxes after the poling field has been removed. Thus, it is necessary to investigate the decay of the second order effect so that material's stability my elucidated. Shown in Fig. 8 is the relaxation of the LEA response for a 2.5 wt%

DR1/PMMA film. This measurement was performed at 80 °C using an insitu poling technique. In the LEA relaxation experiment both the intensity at the modulation frequency (Ω) of the applied electric field (I^{Ω}) and the intensity of the chopped light (I_o) are simultaneously measured. The sample is fixed at an angle of 20° in order to maximize the LEA single. The real part of the zero field refractive index, the applied modulated electric field, and optical wavelength were all kept constant. Initially, the sample film was heated to 80° slowly and allowed to equilibrate. After the sample temperature had stabilized, a large (about $1.2*10^6$ V/cm) static (DC) electric field is applied to the film to orient the NLO chromophores. After allowing suitable time for poling, the poling (DC) field is removed. At this time the modulated intensity and the transmitted light intensity are monitored in real time as seen in Fig. 8. One notes the intensity of I^{Ω} decreases with increasing time, indicating that the NLO chromophores relax back to their original random orientation. We now compare the relaxation of the LEA intensity with the relaxation of the second harmonic generation intensity.

The orientational relaxation in poled second order polymeric materials is generally probed by the second harmonic generation (SHG) technique.[26] The apparatus for this experiment is shown in Fig. 4. A typical SHG poling and relaxation curve measured at 90 °C for a 2.5 wt% DR1/PMMA is shown in Fig. 9. This measurement was also performed using the contact poling method with a field of about $1.2*10^6$V/cm. Detailed experimental procedures for the SHG relaxations measurements have been published elsewhere.[22,23,30] As it can be seen from Fig.9 the SHG intensity reaches a steady value before the poling field is terminated. At this time the SHG decay is monitored at the equilibrated temperature.

Shown in Figs. 10 and 11 are the fitted relaxation curves for the LEA and SHG decay measurements obtained for a 2.5 wt% DR1/PMMA film at 80°C. The relaxation of the LEA effect and the SHG signal is fit to the stretched two Kohlraush-Williams-Watts exponential functions,[30]

$$d_{33} = \frac{1}{2}\chi_{33}^{(2)} = a e^{-(t/\tau_1)^{\beta_1}} + b e^{-(t/\tau_2)^{\beta_2}} \qquad (19)$$

In this expression τ_1 and τ_2 are the two relaxation time constants, β_1 and β_2 are the parameters describing the width of the distribution of relaxation times, and a and b correspond to the magnitude of the intensity associated with each particular stretched exponential. In both cases (LEA and SHG) the β values obtained from the fit are close to unity. Due to the experimental configuration of applying the poling (DC) field and applying the modulated field (AC), the first few points of the relaxation process in the LEA measurement were lost. However, it has been shown elsewhere that the first relaxation time τ_1 (the beginning of the decay curve) is associated with certain mechanisms, such as switching off of the electrodes and surface charge removal, and the third order optical effect which do not particularly relate to the relaxation of the NLO chromophores.[15,22,23] Strong evidence has shown that the first time constant is not significantly effected by temperature.[22] However, the second time constant τ_2 is very temperature dependent and is related to the relaxation of the NLO chromophores back into the polymer matrix.[22,23,28,29] The relaxation time (τ_2) for the LEA measurement is found to be 680 s and 735 s for the SHG relaxation

curve obtained under the same experimental conditions.

The two different techniques produce relaxation times of similar magnitudes. However, the relaxation times are not identical. Although there are small systematic errors in the measurements, there may be other reasons why the two curves do not render the same time constant.[31] The field induced polar order probed in the LEA measurement is an incoherent process involving the transition dipole moment of the NLO chromophores. The small modulation of the imaginary part of the refractive index (n_I) results in a significant modulation of the absorption coefficient. Conversely, the SHG measurement is a coherent process which is associated with the dipole moments of the ground and excited states as well as the transition dipole moment. Although both of these measurements are sensitive to dipolar reorientation of the NLO chromophore, they may not be affected by the reorientation in the same manner.

Summary and Conclusions

The linear electro-absorption and electro-optic techniques have been used to gain information concerning the complete characterization of the second order effect in a model guest/host system. The LEA measurement has been used to measure the imaginary part of the linear electro-optic effect near and far from resonance. The Dispersion of the LEA has been measured for the DR1/PMMA film and shifts in the maximum and bandshape have been interpreted as due to the linear Stark effect and dipolar orientation. Expressions for obtaining real and imaginary Pockels coefficients using the LEA and LEO experimental data

are provided. The second harmonic generation technique has been used as a comparison to the relaxation of the LEA response. From the fitted curves of the two different measurements (SHG and LEA), relaxation times of similar magnitudes have been obtained. We have demonstrated the usefulness of the LEA technique for the characterization of the second order nonlinear optical properties of organic polymeric materials.

Acknowledgments

We thank the office of Naval Research for support of this work.

References

1) J. Cities, P. Ashley, R. Leavitt Appl. Phys. lett. **68**, 11, 1452, 1996.

2) F. Kajzar, J. Messier, Phys.Rev. **A32**, 2352, (1985).

3) C.E. Masse, J.L. Conroy, S.K. Tripathy J.of Appl. Polymer Science, **60**, 4, 513, 1996.

4) S.R. Marder, J.E. Sohn, G.D. Stucky, Materials for Nonlinear Optics: Chemical Perspectives; ACS Symposium Series No.455, (American Chemical Society, Washington D.C. 1991).

5) T. Verbiest, A. Persoons, Macromolecular Symposia, **102**, 347, 1996.

6) A. Jen, T. Chen, Y. Cai, Chemistry of Materials, **8**, 3, 607, 1996.

7) P. Sharma, P. Zhou, H. Frish, J. Polymer Science, part A, **34**, 6, 1049, 1996.

8) H. Xie, X. Huang, J. Guo, J. of Appl. Polymer Science, **60**, 4, 537, 1996.

9) A. Sinha, B. Mandal, L. Chen, Macromolecules, **28**, 16, 5681, 1995.

10) A. Suzuki, Y. Masuoka, J.Appl.Phys., **77**, 3, 965, 1995.

11) R. Jeng, G. Hsiue, S. Tripathy, J. Appl. Polymer Science, **55**, 2, 209, 1995.

12) L. Sooman, B. Park, Y. Kim, Optical and Quantum electronics, **27**, 5, 411, 1995.

13) J. Jerphagnon, S. K. Kurtz, J.Appl.Phys. **41**, 41, 1667, 1970.

14) Loucif-Saibi, R.; Nakatani, R.K.; Delaire, J.A.; Dumont, M.; Sekkat, Z. Chem. Mater. **1993**,5,229.

15) Stahelin, M.; Walsh, C.A.; Burland, D.M.; Miller, R.D.; Twieg, R.J.; Volksen, W. J.Appl.Phys. **1993**,73,8471.

16) Craig, G.S.; Cohen, R.E., Schrock, R.R.; Esser, A.; Schrof, W.; Macromolecules **1995**,28,2512.

17) Burland, D.M.; Miller, R.D.; Walsh, C.A. Chem. Rev. **1994**,94,31.4)

18) J.L. Bredas, C. Adant, A. Persoons, A.Chem.Rev. **94**, 243, (1994).

19) D.S. Chemla, J. Zyss, Nonlinear Optical Properties of Organic Molecules and Crystals (Academic Press, Orlando, 1987).

20) P.N. Prasad, D.J. Williams, Introduction to Nonlinear Optical Effects in Molecules and Polymers (Wiley, New York, 1991).

21) Metricon apparatus is used to measure the real part of the refractive index.

22) Goodson, T.; Gong, S.S; Wang, C.H. Macromolecules **1994**,27,4278

23) Goodson, T.; Wang, C.H.; J.Appl.Phys. 1996, 79, 3, 1267.

24) S. Jeglinski, Z.V. Verdeny, Synth.Met. **49-50**, 509, (1992).

25) B.I. Green, J. Orenstein, R.R. Millard, R.L. Williams, Phys.Rev.Lett. **58**, 2750, (1987).

26) K.D. Singer, Nonlinear Optical Properties of Organic Materials IV; SPIE-Int.Soc.Opt.Eng.: Washington, **1560**, (1991).

27) A. Yariv, P. Yeh, Optical Waves in Crystals; John Wiley & Sons: New York, (1984).

28) H.W. Guan, C.H. Wang, J.Chem.Phys. **98**, (4), 3463, (1993).

29) Gong, S.S.; Goodson, T.; Guan, H.W.; Wang, C.H. Nonlinear Optics **1993**,6,93.

30) Williams, G.; Watts, D.C. Trans. Faraday Soc. **1970**, 66, 80.

31) T. Goodson, C. H. Wang, J.Phys.Chem., (in press)

Table I Electro-optical and electro-absorption data for the 2.5 wt% DR1/PMMA film.

λ(nm)	n_{oR}	n_{oI}	$(n_o^3 r)_R$	$(n_o^3 r)_I$	r_R	r_I	a
488	1.511	0.91	1.23	6.89	1.24	0.16	0.215
514	1.502	0.22	0.55	1.85	0.37	0.41	0.087
632.8	1.489	0.050	0.21	0.050	0.063	0.085	0.28

Figure Captions

Figure 1: The molecular structure of the Disperse Red 1 chromophore.

Figure 2: The linear electro-absorption apparatus.

Figure 3: The linear absorption spectrum of a 2.5 wt% DR1/PMMA film.

Figure 4: The second harmonic generation setup.

Figure 5: The angular dependence of incident light intensity I_0 for a 2.5 wt% DR1/PMMA film.

Figure 6: The linear electro-absorption spectrum of a 2.5 wt% DR1/PMMA film.

Figure 7: The applied field dependence of the LEA signal detected at the modulated frequency Ω for a 2.5 wt% DR1/PMMA film.

Figure 8: The relaxation of the LEA signal for a 2.5 wt% DR1/PMMA film poled at 80°C with a poling field of $1.2*10^6$ V/cm.

Figure 9: The rise and decay curve of the SHG intensity for a 2.5 wt% DR1/PMMA film poled at 90°C with a poling field of $1.2*10^6$ V/cm.

Figure 10: The fitted LEA relaxation curve for a 2.5 wt% DR1/PMMA film measured at 80°C.

Figure 11: The fitted SHG relaxation curve for a 2.5 wt% DR1/PMMA film measured at 80°C.

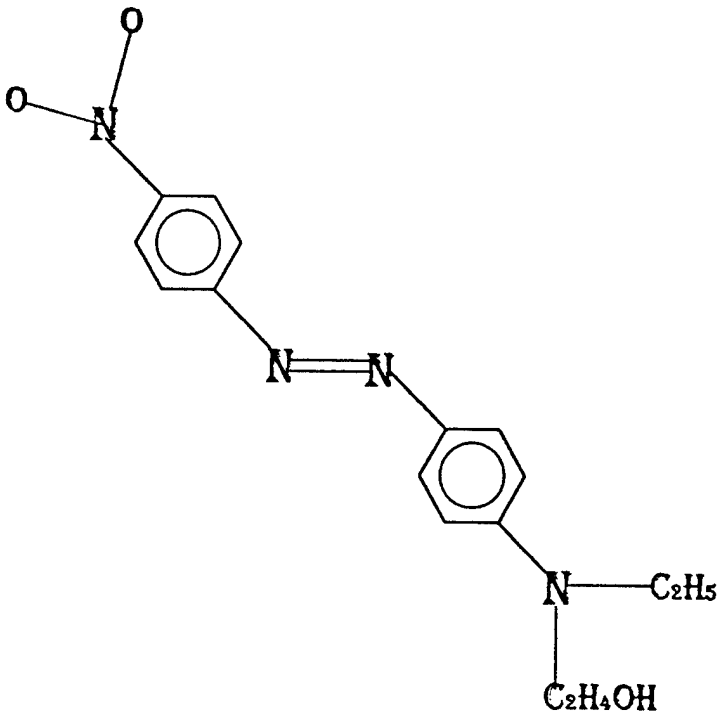
O
O
N
N
N
N
C2H5
C2H4OH

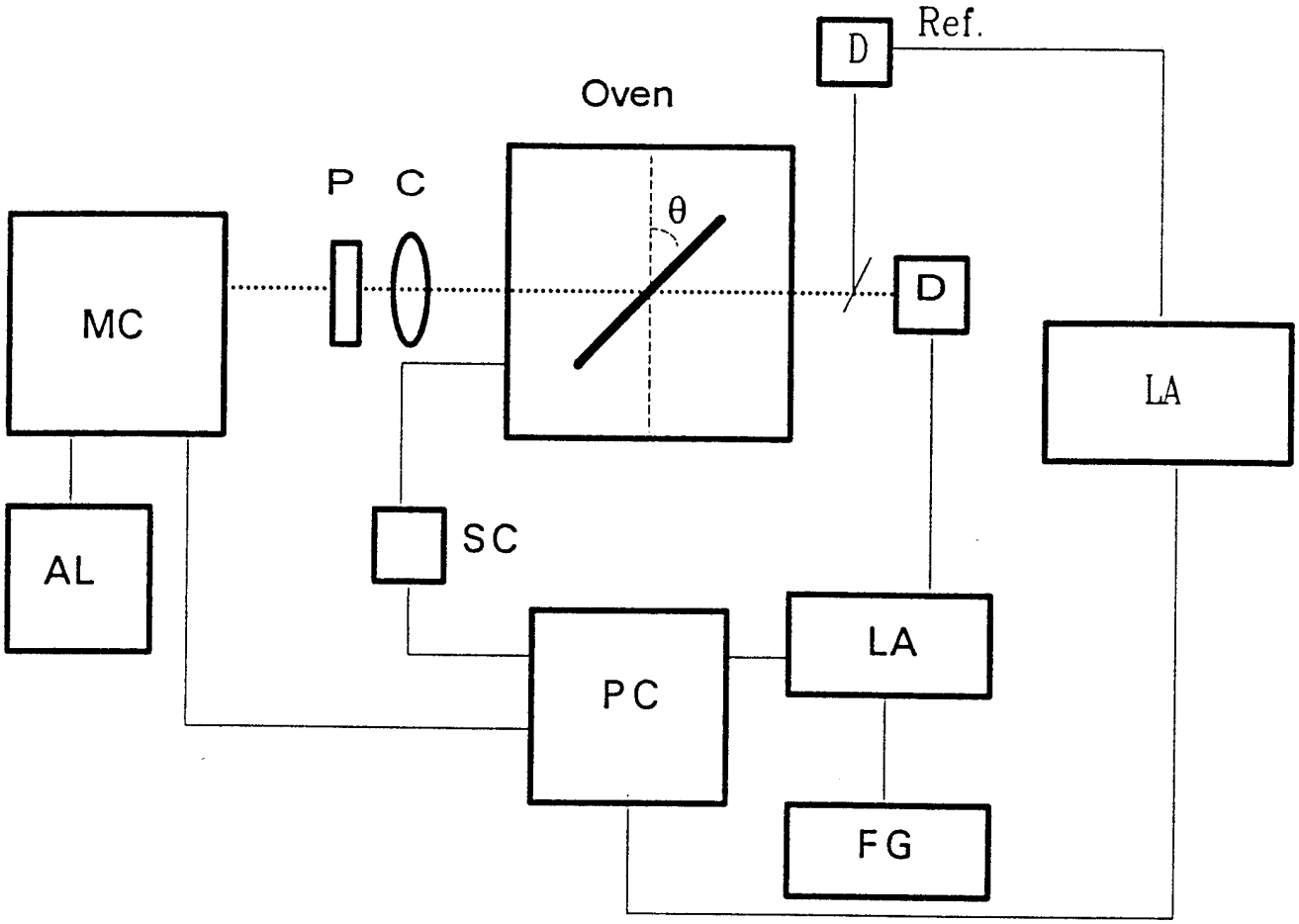
Ref.
D
Oven
P
C
θ
MC
D
LA
AL
SC
LA
PC
FG

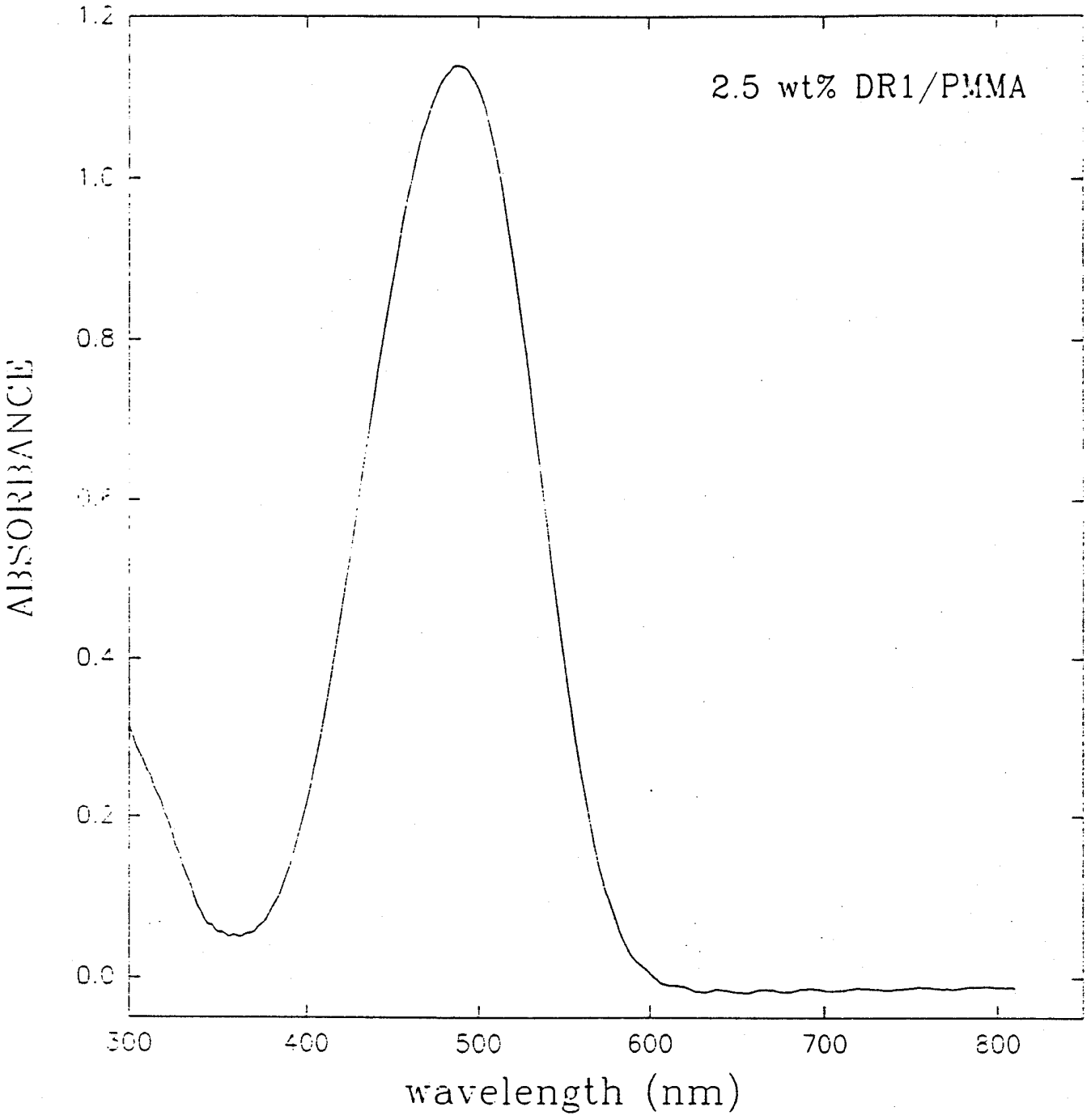
2.5 wt% DR1/PMMA
ABSORBANCE
1.2
1.0
0.8
0.4
0.2
0.0
300
400
500
600
700
800
wavelength (nm)

F. J. 3

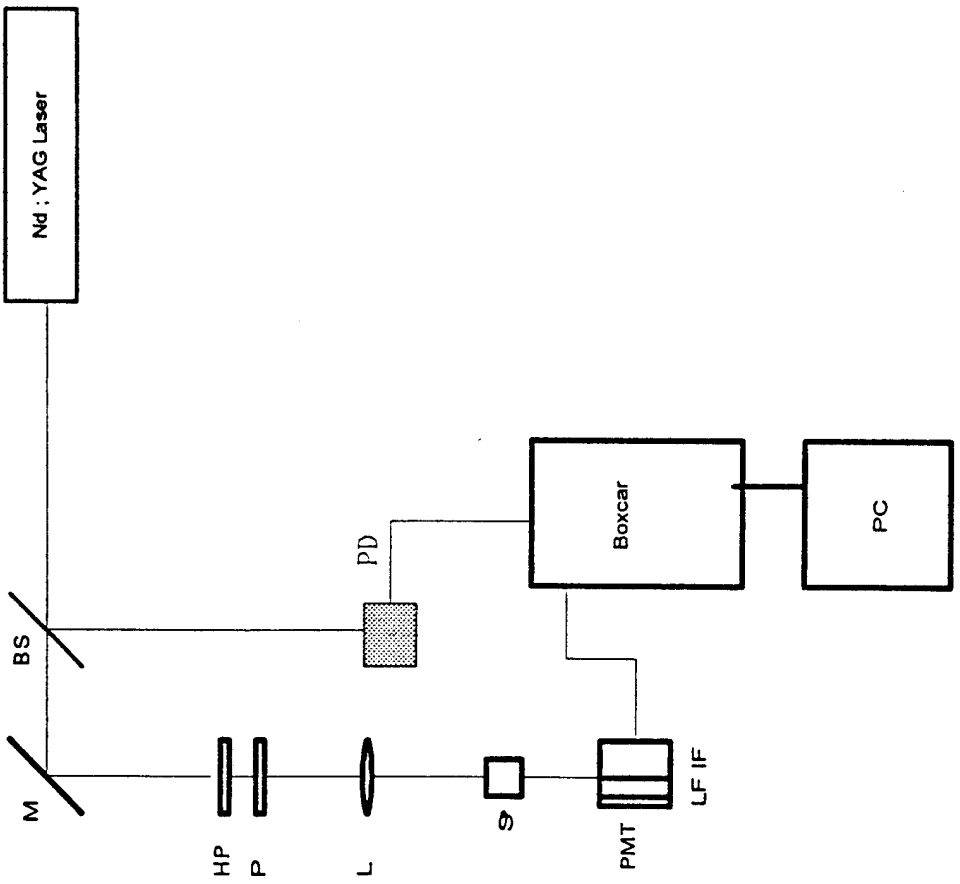

Fig.4

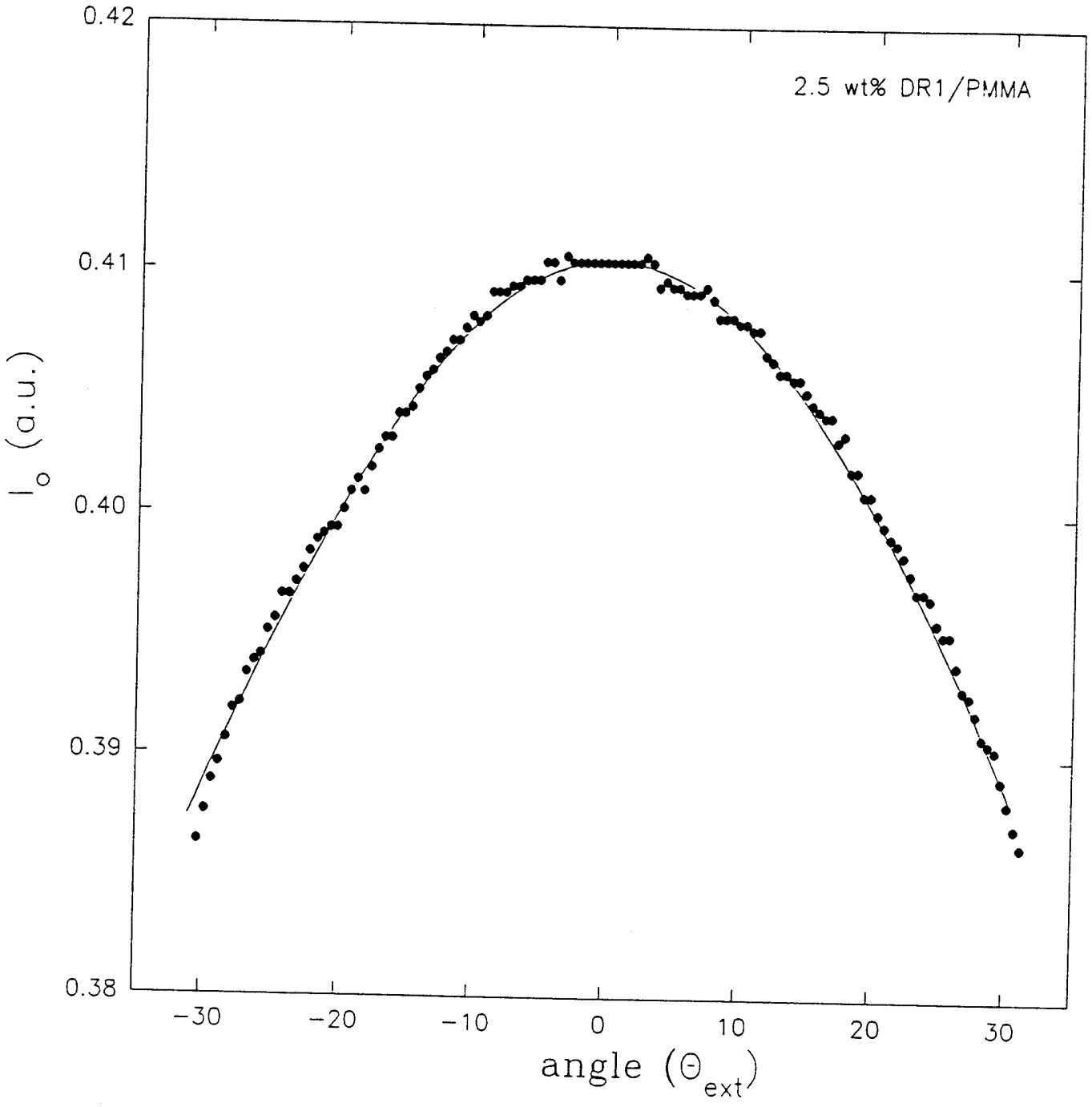
0.42
0.41
0.40
0.39
0.38
2.5 wt% DR1/PMMA
I_o (a.u.)
−30
−20
−10
0
10
20
30
angle (Θ_{ext})

F-T-5

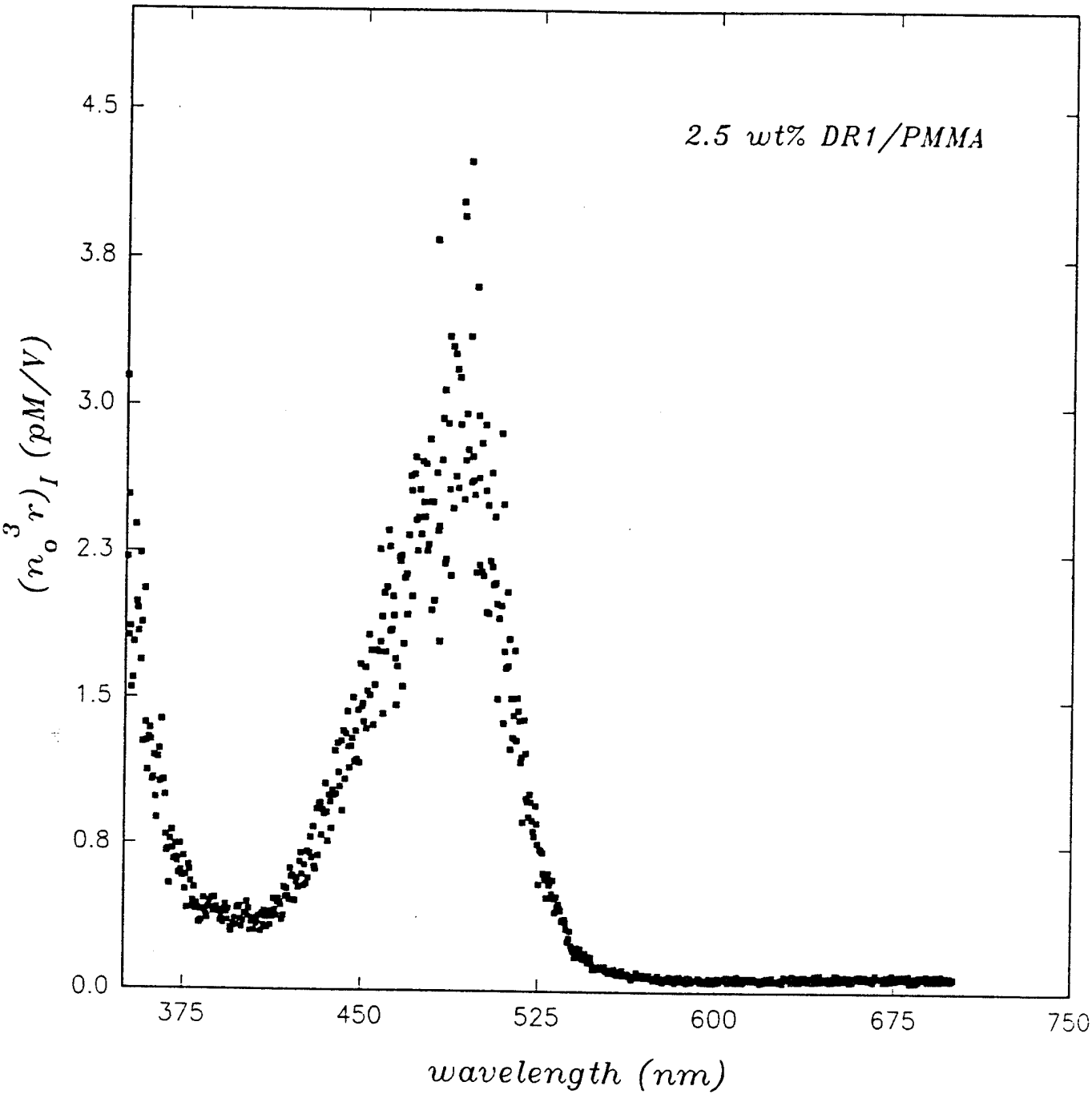
2.5 wt% DR1/PMMA
4.5
3.8
3.0
2.3
1.5
0.8
0.0
$(n_o^3 r)_I$ (pM/V)
375
450
525
600
675
750
wavelength (nm)

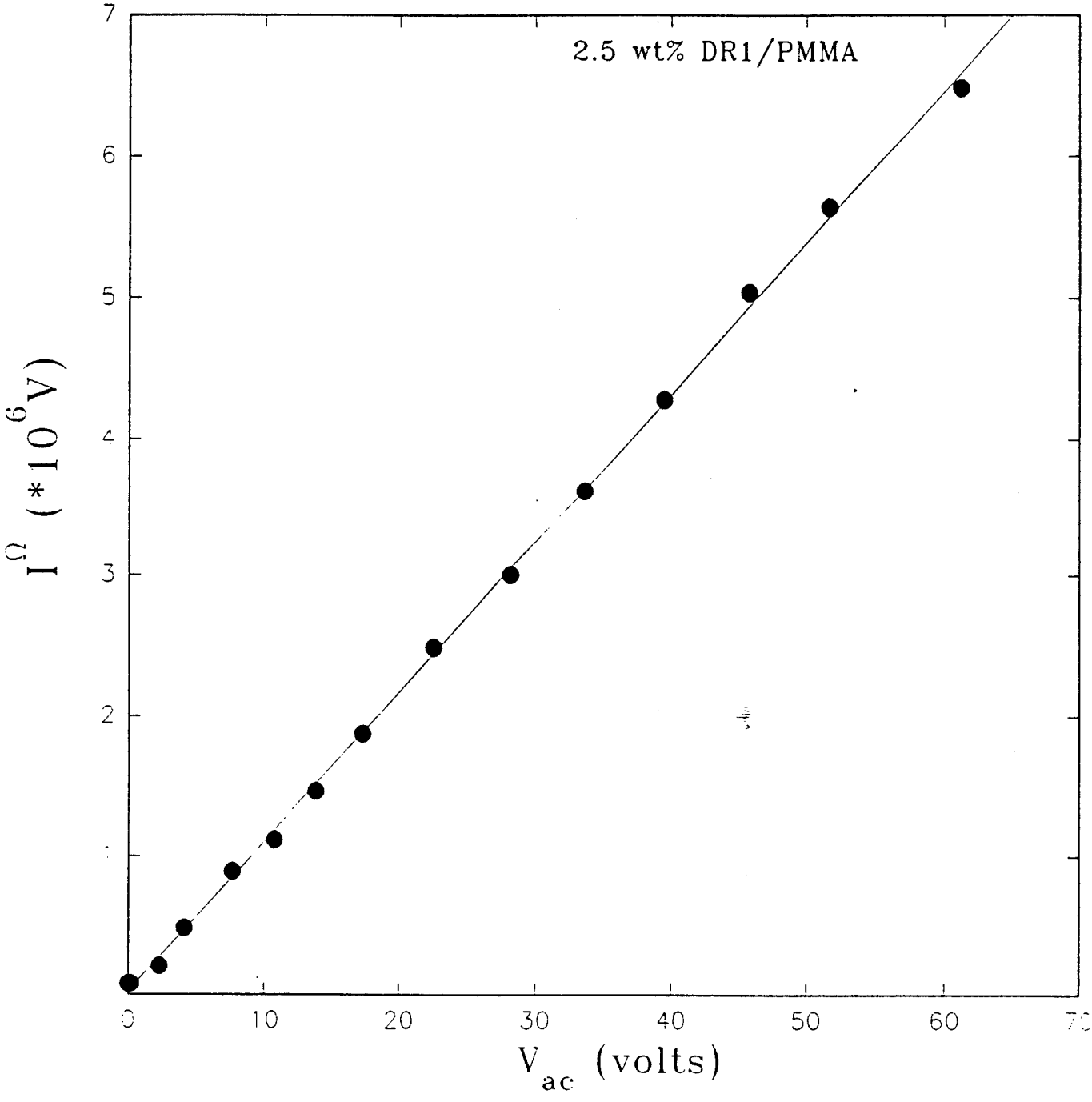

Fig. 7

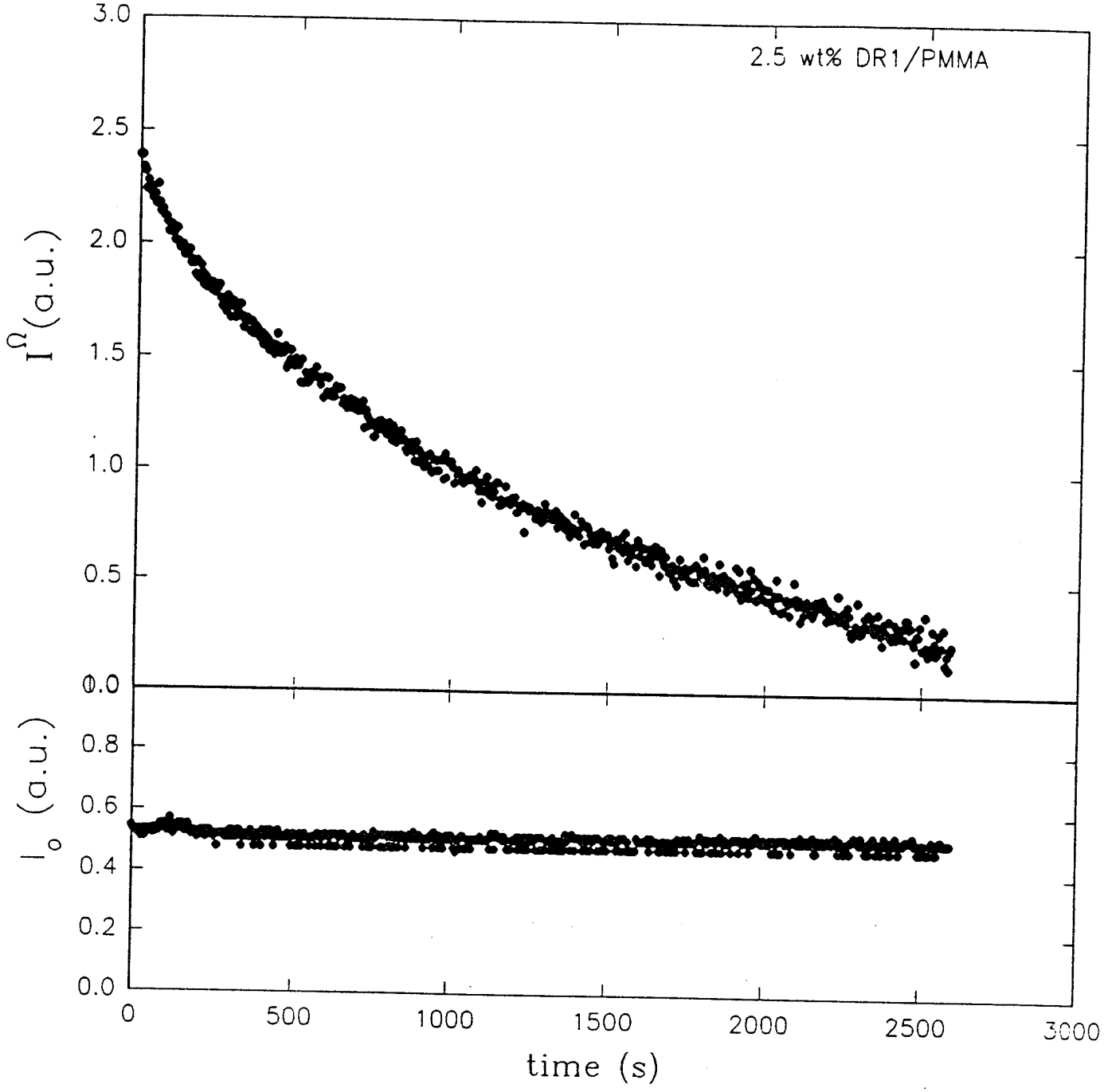
2.5 wt% DR1/PMMA
I^{Ω}(a.u.)
I_o (a.u.)
time (s)
3.0
2.5
2.0
1.5
1.0
0.5
0.0
0.8
0.6
0.4
0.2
0.0
0
500
1000
1500
2000
2500
3000

Fig 8

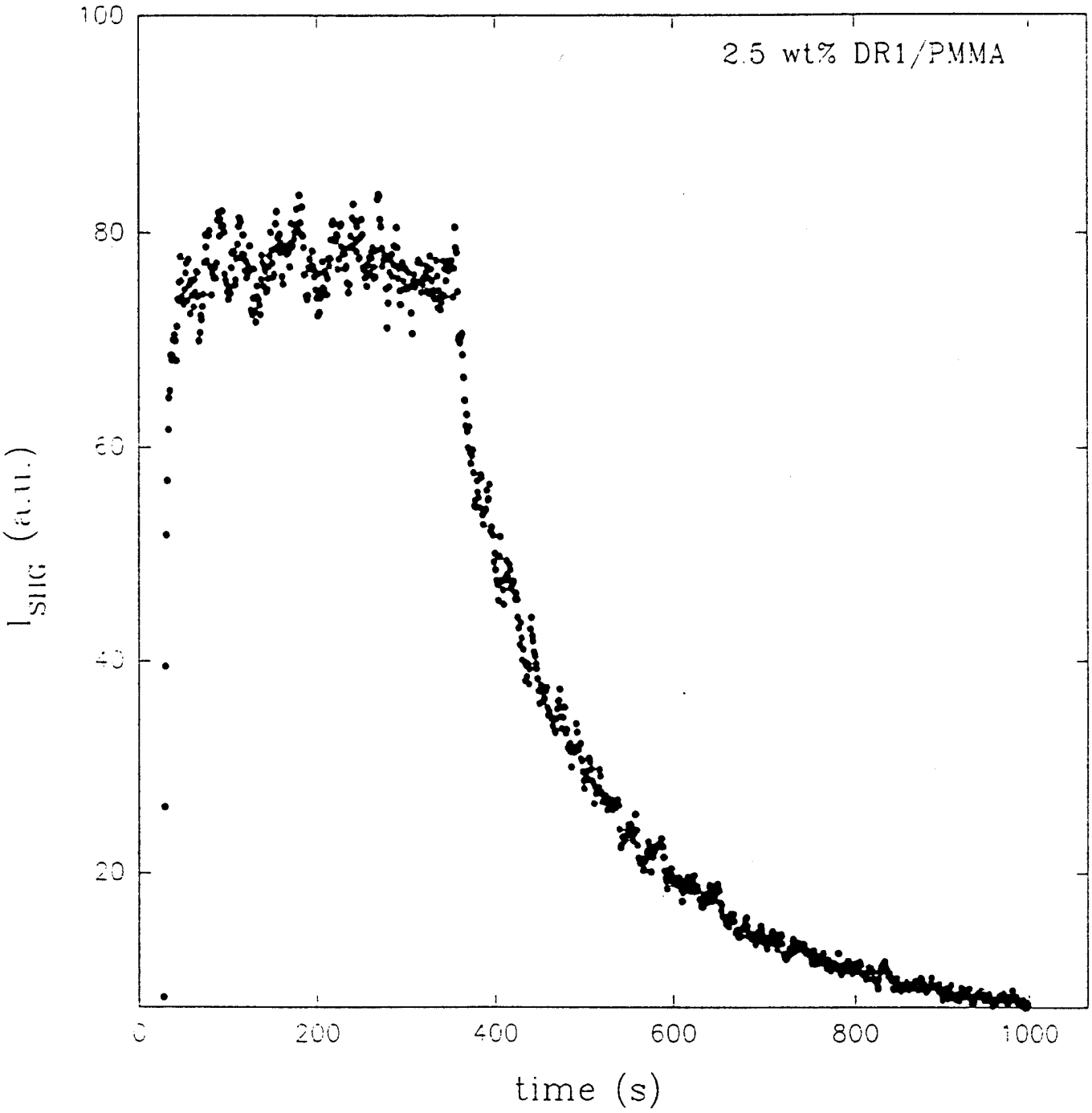
2.5 wt% DR1/PMMA
100
80
60
40
20
0
200
400
600
800
1000
time (s)
I_{SHG} (a.u.)

Fig. 9

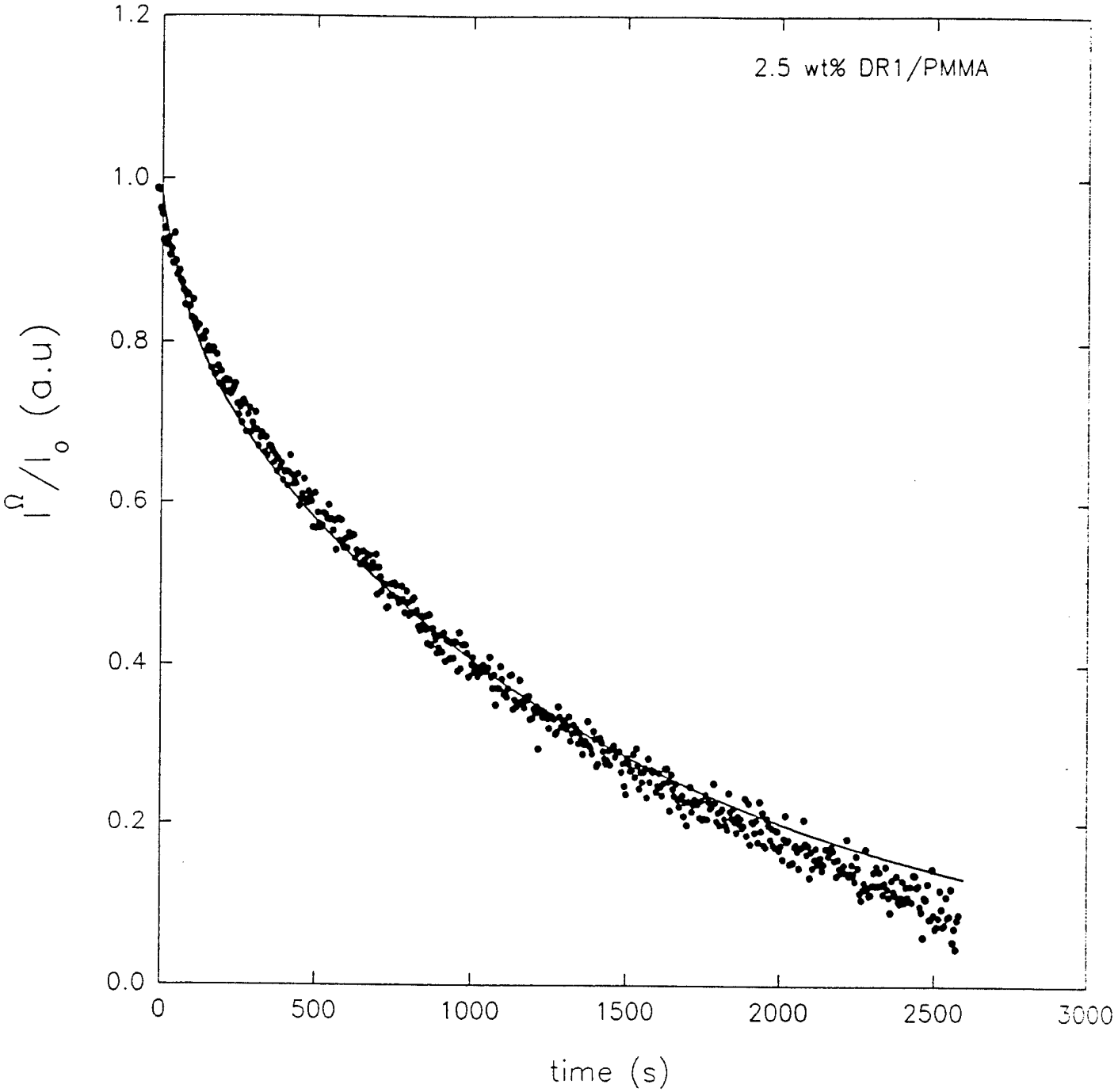
2.5 wt% DR1/PMMA
1.2
1.0
0.8
0.6
0.4
0.2
0.0
0
500
1000
1500
2000
2500
3000
time (s)
I/I0 (a.u)

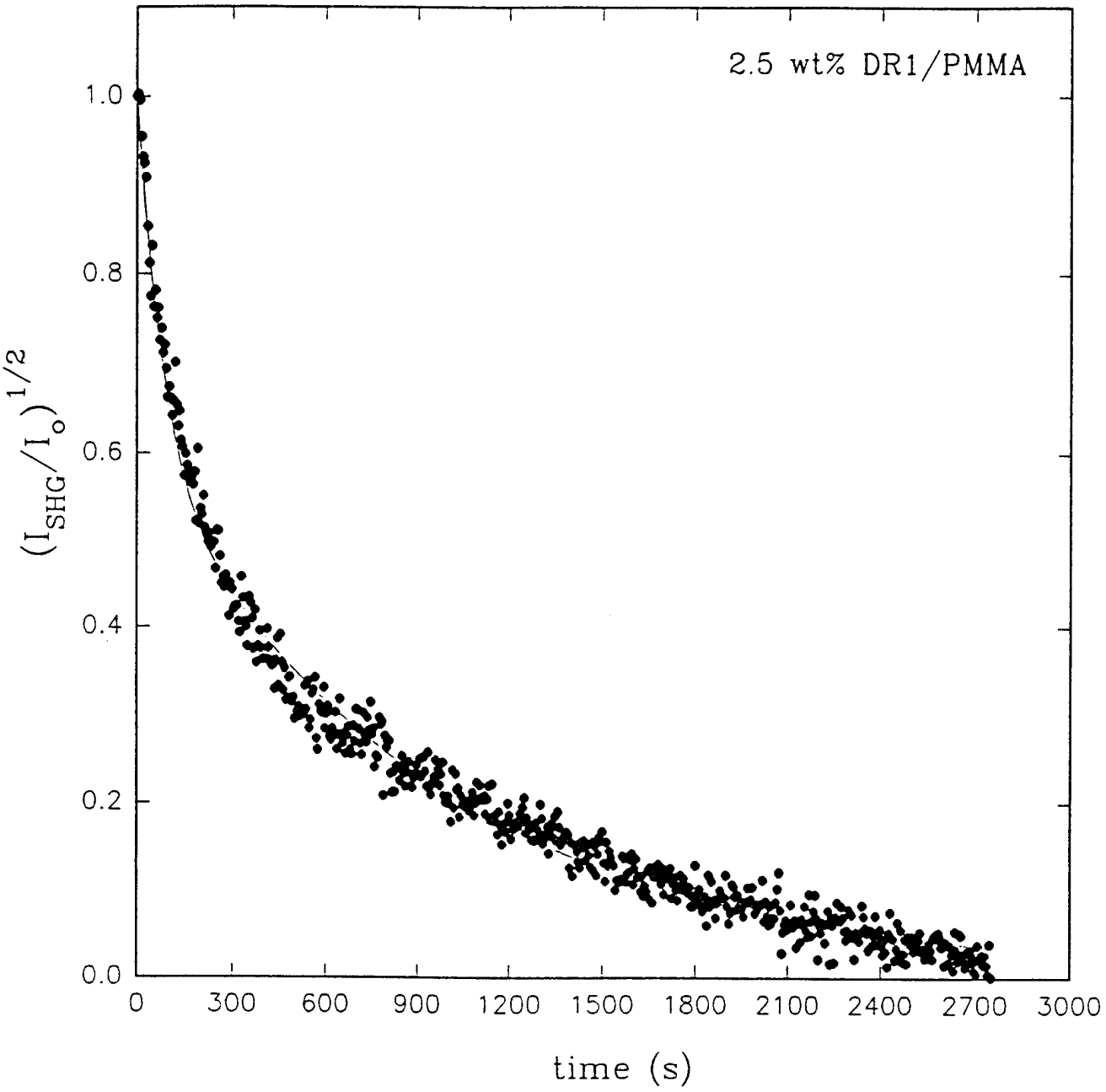
2.5 wt% DR1/PMMA
1.0
0.8
0.6
0.4
0.2
0.0
$(I_{SHG}/I_o)^{1/2}$
0
300
600
900
1200
1500
1800
2100
2400
2700
3000
time (s)

Fig. 11